



## Sea-ice distribution and atmospheric pressure patterns in southwestern Okhotsk Sea since the Last Glacial Maximum

Kota Katsuki<sup>a,b</sup>, Boo-Keun Khim<sup>a,\*</sup>, Takuya Itaki<sup>c</sup>, Yusuke Okazaki<sup>d</sup>, Ken Ikehara<sup>c</sup>, Yuna Shin<sup>e</sup>, Ho Il Yoon<sup>f</sup>, Cheon Yun Kang<sup>f</sup>

<sup>a</sup> Division of Earth Environmental System, Pusan National University, Busan 609-735, Republic of Korea

<sup>b</sup> Center for Advanced Marine Core Research, Kochi University, Japan

<sup>c</sup> Institute of Geology and Geoinformation, Geological Survey of Japan, Japan

<sup>d</sup> Japan Agency for Marine-Earth Science and Technology, Japan

<sup>e</sup> Wonju Regional Environmental Office, Monitoring and Analysis Division, Republic of Korea

<sup>f</sup> Korea Polar Research Institute, Republic of Korea

### ARTICLE INFO

#### Article history:

Received 17 June 2009

Accepted 30 December 2009

Available online 11 January 2010

#### Keywords:

sea-ice

diatom

radiolaria

atmospheric pressure

paleoclimate

Okhotsk Sea

### ABSTRACT

Sea-ice diatom taxa (*Fragilariopsis cylindrus* and *Fragilariopsis oceanica*) and their relative abundance in the Okhotsk Sea were used to reconstruct the history of sea-ice distribution and atmospheric pressure patterns since the Last Glacial Maximum (LGM). The temporal state of sea-ice distribution and atmospheric pressure patterns since the LGM can be divided into three modes: northern Aleutian Low mode, southern Aleutian Low mode, and strong Siberian High mode. The Southern Aleutian Low mode was dominant before 15 ka and after 6.5 ka, respectively, showing expanded sea-ice distribution into the central and southern Okhotsk Sea. During the deglaciation period (15 ka to 10 ka), sea-ice retreated from the southern Okhotsk Sea because of the pronounced westerly winds under the strong Siberian High mode. However, sea-ice distribution expanded in the northern Okhotsk Sea, which favors the development of extensive polynyas on the northern continental shelf. Occurrences of northern Aleutian Low mode were frequent between 10 and 6.5 ka, while sea-ice distribution expanded into the eastern Okhotsk Sea. Formation of the Okhotsk Sea Intermediate Water, inferred from radiolarian species *Cycladophora davisiana*, intensified under both northern Aleutian Low mode and strong Siberian High mode.

© 2010 Elsevier B.V. All rights reserved.

### 1. Introduction

The present-day Okhotsk Sea, located in the southern limits of sea-ice extent in the Northern Hemisphere, is characterized by seasonal sea-ice cover. Sea-ice formation affects seawater density, albedo, and evaporation (Smith et al., 2003) which are crucial factors in forming dense intermediate waters (e.g., Martin et al., 1998). In particular, the mechanism of sea-ice extent and decay in the Okhotsk Sea is governed by atmospheric circulation around the Arctic Ocean (e.g., Rikiishi and Takatsuji, 2005). Furthermore, the present-day Okhotsk Sea plays an important role as the direct ventilation source for the North Pacific Intermediate Water (NPIW) (Yasuda, 1997). Rapid advance and retreat of sea-ice and the degree of intermediate water formation are regarded as significant controlling factors for global paleoclimatic conditions (e.g., Gorbarenko et al., 2007b). Therefore, better knowledge of sea-ice distribution in the Okhotsk Sea can greatly assist the

understanding of paleoclimate change with respect to the atmospheric pressure systems.

Distribution patterns of microfossil diatoms and radiolarians are strongly influenced by seawater hydrographic conditions such as nutrient availability, salinity, and dissolved oxygen concentration. Diatoms are by far the most abundant plankton in the Okhotsk Sea (Sorokin and Sorokin, 1999). Diatoms, as important primary producers, have also been used as environmental proxy for the reconstruction of surface-water conditions (e.g., Shiga and Koizumi, 2000). In contrast to surface-water dwelling diatoms, siliceous radiolarians live at various depths throughout the water column. Hence, radiolarian fossil assemblages are often used to reconstruct vertical water-mass structures (Nimmergut and Abelmann, 2002; Matul et al., 2003; Abelmann and Nimmergut, 2005; Okazaki et al., 2006; Itaki et al., 2008).

In addition to oceanographic investigations (e.g., Martin et al., 1998; Itoh et al., 2003), paleoenvironmental and micropaleontological studies have also been accomplished successfully in the Okhotsk Sea (e.g., Gorbarenko, 1996; Keigwin, 1998; Shiga and Koizumi, 2000; Ternois et al., 2001; Narita et al., 2002; Seki et al., 2003, 2004a,b; Okazaki et al., 2005, 2006; Harada et al., 2006; Sakamoto et al., 2006;

\* Corresponding author. Tel.: +82 51 510 2212; fax: +82 51 581 2963.  
E-mail address: [bkkhim@pusan.ac.kr](mailto:bkkhim@pusan.ac.kr) (B.-K. Khim).

Gorbarenko et al., 2007a,b; Itaki et al., 2008). According to above cited reports, paleoenvironmental changes in the Okhotsk Sea are regionally specific. In particular, paleoenvironmental changes in the southern Okhotsk Sea have received increasing attention during the last 5 years, including Holocene sediment studies (Kawahata et al., 2003; Shimada et al., 2004; Itaki and Ikehara, 2004; Okazaki et al., 2005; Harada et al., 2006; Sakamoto et al., 2006, Itaki et al., 2008). Temporal and spatial distribution of sea-ice in the Okhotsk Sea since the Last Glacial Maximum (LGM) was demonstrated by Shiga and Koizumi (2000) and Sakamoto et al. (2005). They showed sea-ice distribution changes along the east–west transect in the central Okhotsk Sea. However, information on historical sea-ice status along the north–south transect remains porous and limited only to data presented by Shiga and Koizumi (2000). Therefore, in order to compile information on sea-ice distribution patterns in the entire Okhotsk Sea since the LGM, comparative data of fossil assemblages from the literature were integrated with newly presented data in this study.

Here we document the absolute and relative abundance changes of fossil siliceous plankton assemblages in piston cores (GH00-1002 and MD01-2412) from the southwestern Okhotsk Sea (Fig. 1) for the purpose of elucidating historical sea-ice cover and atmospheric pressure conditions.

## 2. Oceanographic setting

The Okhotsk Sea is one of the many typical marginal seas in the northwest Pacific (Fig. 1). Sea-ice formation in the Okhotsk Sea is caused by an influx of freshwater from the Amur River as well as the strong westerly to northwesterly cold winds during the winter, derived from interaction between the Siberian High (SH) and Aleutian Low (AL) pressure systems (Martin et al., 1998; Wong et al., 1998). In winter, the robust SH pressure occupies the Asian continent with strong AL pressure to its east. The AL pressure dominates the northern North Pacific from late fall to spring of the next year. The intensity and position of these pressures are associated with air circulation around the Arctic Ocean (Kutzbach, 1970). The inter-annual variability of the AL pressure system during the 20th century was on the decadal scale, lasting at least three winters in each decade. This variability is not only associated with the Arctic Oscillation but also with the Pacific–North America Pattern (Overland et al., 1999). Inter-annual variability of sea-ice distribution is mainly controlled by atmospheric conditions including air temperature and geostrophic wind (Kimura and Wakatsuchi, 2004). Such inter-annual variability is negatively correlated with the amount of freshwater discharge from the Amur River (Ogi and Tachibana, 2006). The inflow of warm freshwater tends

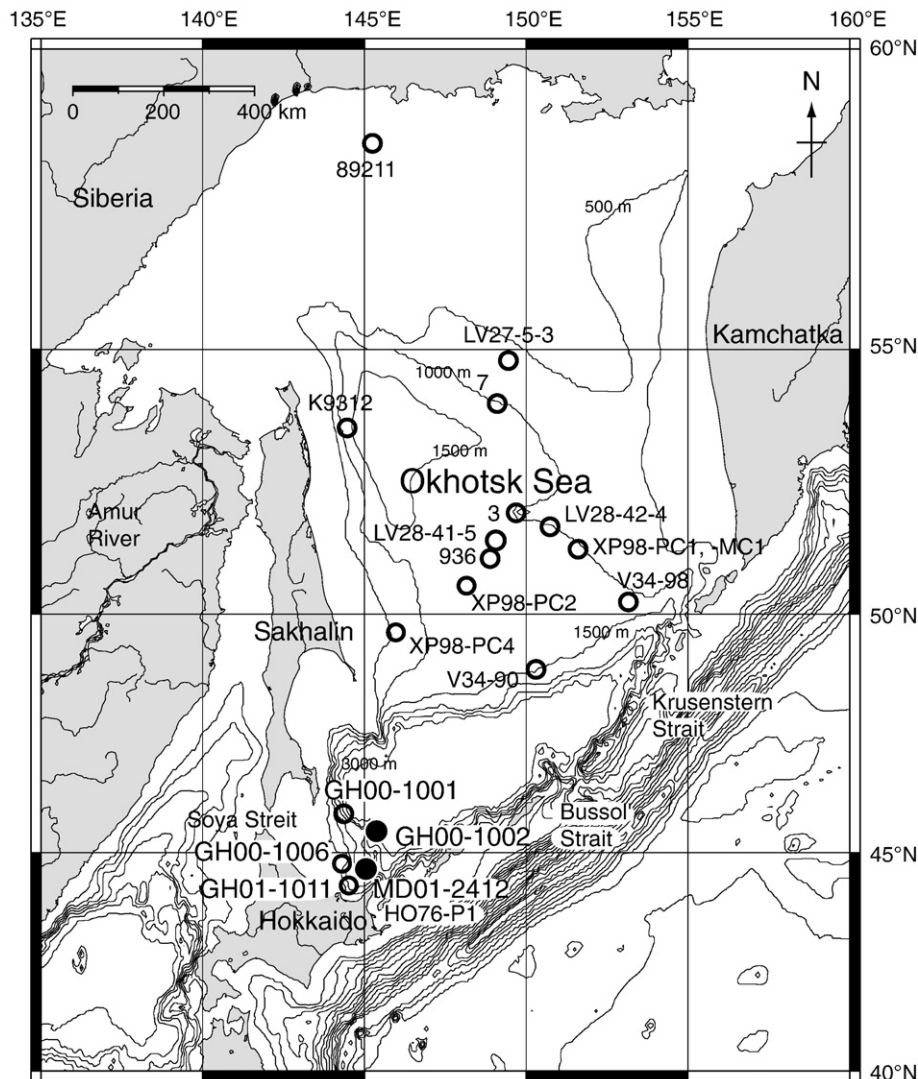


Fig. 1. A map showing the bathymetry of study area with locations of sediment cores in this study (GH00-1002 and MD01-2412: solid circles) and previously published reports (open circles). The map was drawn by Online Map Creation.

to raise sea-surface temperature, which subdues sea-ice formation in the following winter.

The Okhotsk Sea is a direct ventilation source for the NPIW, named Okhotsk Sea Intermediate Water (OSIW) (Talley, 1991). The OSIW properties are characterized by the lowest salinity and the highest dissolved oxygen content on the 26.8 ( $\sigma_\theta$ ) isopycnal surface in the North Pacific. The OSIW between 200 and 1000 m depth can be divided into two parts: upper OSIW from 200 to 500–600 m, and lower OSIW from 500–600 m down to 1000 m (Wong et al., 1998). The cold, fresh and oxygen-rich water is formed by mixing of Dense Shelf Water (DSW), Soya Warm Current (SWC) water, and North Pacific Water (NPW) (Talley, 1991; Watanabe and Wakatsuchi, 1998). Brine rejection with sea-ice formation in winter produces the DSW on the northern continental shelf in the Okhotsk Sea, which is cold and oxygen-rich, but relatively less saline (Watanabe and Wakatsuchi, 1998). The DSW is a main ventilation source in the Okhotsk Sea (Alfultis and Martin, 1987). The SWC water, flowing out through the Soya Strait (Fig. 1) from the East/Japan Sea, is warm, saline, and oxygen-rich, and also contributes to the formation of the OSIW (Talley, 1991).

### 3. Materials and methods

Two piston cores GH00-1002 (45°11'N, 144°27'E; water depth: 922 m; core length: 473 cm) and MD01-2412 (44°32'N, 145°00'E; water depth: 1225 m; core length 52.69 m) were collected off Hokkaido in the southwestern Okhotsk Sea during GH00 Cruise of R/V Hakurei-Marui in 2000 and during the IMAGES WEPAMA 2001 Cruise of R/V Marion Defresne, respectively (Fig. 1). Both sediment cores were primarily composed of dark gray silty-clay, intercalated with some volcanic ash layers.

Diatom assemblage was analyzed for 48 samples from core GH00-1002 and 38 samples from core MD01-2412. For core GH00-1002, wet sediments (50 mg) were placed in a beaker with hydrogen peroxide and hydrochloric acid, and left to stand for 24 h. The samples were ultrasonicated for about 15 s in order to homogenize the suspension. Slides were settled on the platform above the bottom of beaker. The beakers were left in an oven for a day in order to let the grains settle on the slides, and for the water to evaporate. These slides were then mounted on glass slides using Canada Balsam. For core MD01-2412, a wet sample was accurately weighed and treated with 10% hydrogen peroxide, 1 N hydrochloric acid, and Calgon® (hexametaphosphate, surfactant). The sample was filtered through a Gelman® membrane filter of 47 mm in diameter with a nominal pore size of 0.45  $\mu$ m. The dried filter samples were permanently mounted on microslides with Canada Balsam following the method described by Okazaki et al. (2005).

All diatoms were identified and counted until the number of individual specimens reached 250 in total. Specimens representing more than half of a valve were counted as 1; for pinnate diatoms, each pole was counted as 1/2. Counts were converted to percentages of total assemblage. Observation with a light microscope was conducted at 600 to 1000 $\times$  magnification. Taxonomical names were standardized by Hasle and Syvertsen (1996). *Nitzschia cylindrus* (Grunow) Hasle and *Nitzschia grunowii* Hasle were transformed into *Fragilariopsis cylindrus* (Grun) Krieger and *Fragilariopsis oceanica* (Cleve) Hasle, respectively.

Radiolarian assemblage was analyzed for 47 samples from core GH00-1002 and 44 samples from core MD01-2412. Sediment samples were treated with hydrogen peroxide and hydrochloric acid to remove carbonate and organic matters, and passed through a sieve with 45- $\mu$ m mesh opening to remove fine particles and enrich radiolarians. All grains, extracted using pipette for core GH00-1002 and filtered through Gelman® membrane filters with a nominal pore size of 0.45 mm for core MD01-2412, were mounted onto glass slides with Canada Balsam. Radiolarians were observed and identified under

an optical microscope at 100 to 200 $\times$  magnification. Detailed analytical procedures are provided by Okazaki et al. (2005), Itaki (2006), and Itaki et al. (2008).

Age model establishments for core GH00-1002 and core MD01-2412 are reported by Itaki et al. (2008) and Sakamoto et al. (2006), respectively. No  $^{14}$ C age measurements using foraminiferal tests were performed on core GH00-1002 because of poor carbonate preservation. Age model for core GH00-1002 was constructed mainly on the basis of tephrostratigraphy (Kawamura et al., 2007) and bulk organic carbon (BOC)-based  $^{14}$ C ages. Linear sedimentation rate between the upper 2 points of the BOC-based  $^{14}$ C ages intersects at 3800 yrBP of the volcanic ash Ta-a (1739 AD). Therefore, we assumed that the BOC-based  $^{14}$ C ages of core GH00-1002 are about 3600 years older than the true age. Based on this assumption, the bottom of GH00-1002 core was estimated to be about 19 ka. The age model for core MD01-2412 was constructed on the basis of  $\delta^{18}$ O stratigraphy of benthic foraminifera (*Uvigerina* spp.), AMS  $^{14}$ C dating of planktonic foraminifera (*Neogloboquadrina pachyderma*, sinistral), and tephrochronology, which were reported by Sakamoto et al. (2006).

### 4. Results

Total diatom valves (number valves  $g^{-1}$ ) gradually increased since 10.5 ka (zone 2), and showed remarkably high values after 5.3 ka (zone 1) in core GH00-1002 (Fig. 2a), which follows similar variation in biogenic opal contents (Fig. 2b). Variation of total diatom valves in core MD01-2412 is similar to that of core GH00-1002, showing an increase since 8.5 ka (zone 2), and remarkably high values since 4.5 ka (zone 1) (Okazaki et al., 2005). Relative abundances of diatom taxa *Fragilariopsis cylindrus* and *F. oceanica* in core GH00-1002 are shown in Fig. 3a. The ice-related diatom species in both cores were second in significant constituents, comprising up to 10% in abundance. The % of *F. cylindrus* was relatively high (over 1%) at 18.8 ka, between 15.1 and 15.9 ka (zone 4), between 13.4 and 13.8 ka (zone 3), at 8.4 ka (zone 2), and since 6.7 ka (zone 1).

The % of *F. oceanica* was also high (over 1%) since 6.7 ka (zone 1). This taxon had increased to over 1% before 18.4 ka (zone 4), between 15.9 and 17.2 ka (zone 4), at 15.0 and 13.8 ka (zone 3), at 9.7 and 7.9 ka (zone 2). In core MD01-2412, the % of *F. cylindrus* was over 1% before 9 ka (zone 3), and greater than 5% before 17 ka (zone 4). Furthermore, the % of *F. oceanica* was almost similar in pattern to *F. cylindrus* with a relatively high value (over 2%) before 17 ka (zone 4) (Fig. 3b). The % of *Fragilariopsis* reported from previous studies is shown in Figs. 3c–h, and the list of cited data sources is presented in Table 1 with radiolarian and IRD data sources.

Variation in relative abundances of radiolarian *Cycladophora davisiana* was significantly high through the cores: 20 to 80% in core GH00-1002 (Fig. 4a) and 1 to 70% in core MD01-2412 (Fig. 4b). In core GH00-1002, *C. davisiana* increased gradually from 28.8 to 80.0% until 8.9 ka, and subsequently decreased gradually to 50.8% until 1 ka. However, in core MD01-2412, *C. davisiana* exhibited abrupt abundance change in the each period. Average *C. davisiana* abundance was 49.1% between 15 and 20 ka, 66.8% between 15 and 6 ka, and 39.8% between 6 and 2 ka. This species indicated extremely low abundance since 1 ka in core GH00-1002 and between 1 and 2 ka in core MD01-2412 (zone 1).

### 5. Discussion

#### 5.1. History of sea-ice distribution based on diatom abundance

Sea-ice distribution patterns have been reconstructed using the relative abundances of sea-ice related diatoms *F. cylindrus* and *F. oceanica* (Hasle, 1990) in sediment cores (e.g., Sancetta, 1983). They belong to the member of ice flora living in waters between  $-1$  and  $3$  °C in temperature (Horner and Alexander, 1972) and their

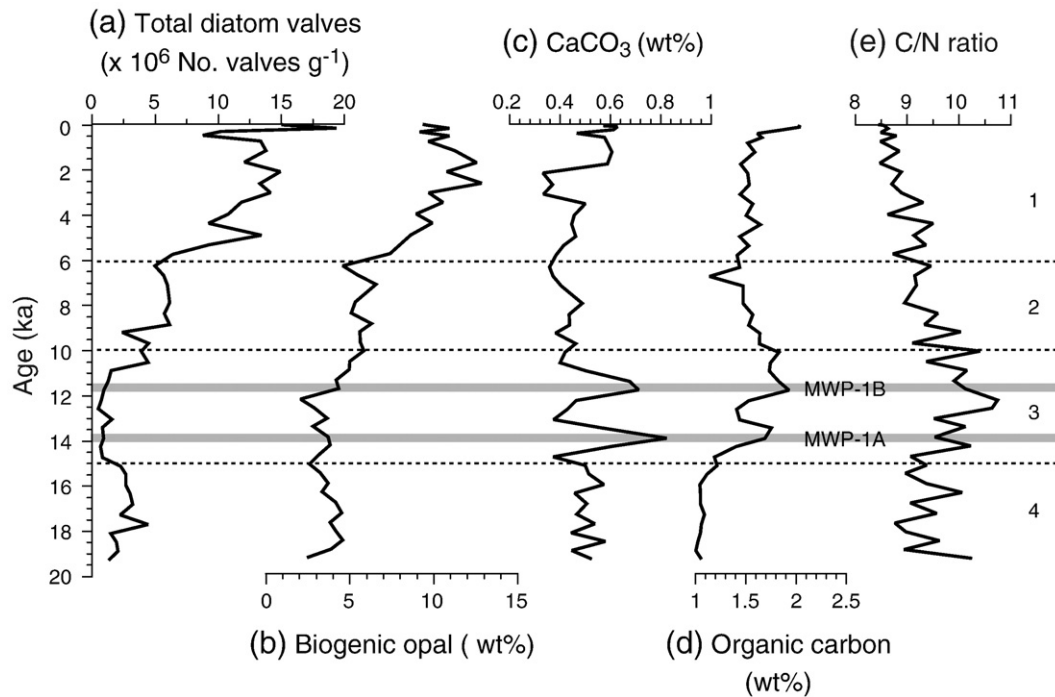


**Fig. 2.** Downcore profiles of the number of (a) total diatom valves, (b) biogenic opal, (c)  $\text{CaCO}_3$ , (d) organic carbon, and (e) C/N in core GH00-1002 (geochemical data were taken from Itaki et al., 2008). The right numbers indicate temporal stages divided into zone 1: Late Holocene (after 6.5 ka), zone 2: Mid-Holocene (6.5–10 ka), zone 3: Deglaciation (10–15 ka), and zone 4: LGM (before 15 ka).

geographic distributions almost overlap with sea-ice distribution in the subarctic Pacific (Sancetta, 1982). In fact, the other sea-ice related diatoms, *Bacterosira bathyomphala*, *Thalassiosira antarctica*, and *Thalassiosira nordenskiöldii*, also appear in every layer of Okhotsk Sea core sediments except for the few layers during the late Quaternary (Shiga and Koizumi 2000; Koizumi et al., 2003; Shimada et al., 2004; Okazaki et al., 2005; Gorbarenko et al., 2007a). This indicates that sea-ice occasionally covered all of the Okhotsk Sea during each stage of the late Quaternary. However, the frequency has been, of course, different. Thus, the temporal distributions of these sea-ice related

diatoms are also different. In particular, *T. antarctica* and *T. nordenskiöldii* often depicted a reversed pattern compared with the other sea-ice related diatoms. The high abundances of *F. cylindrus* and *F. oceanica* in surface sediments indicate that ice cover is present in the spring and early summer. However, the high abundance of *T. nordenskiöldii* occurs under the polynya, which is located in the southern limit of sea-ice cover (Cremer, 1999). Therefore, it is inferred that differences among the distribution patterns of sea-ice related diatoms is dependent on the frequency and duration of sea-ice cover. To reconstruct mean sea-ice distribution in each period since the LGM, we focus our

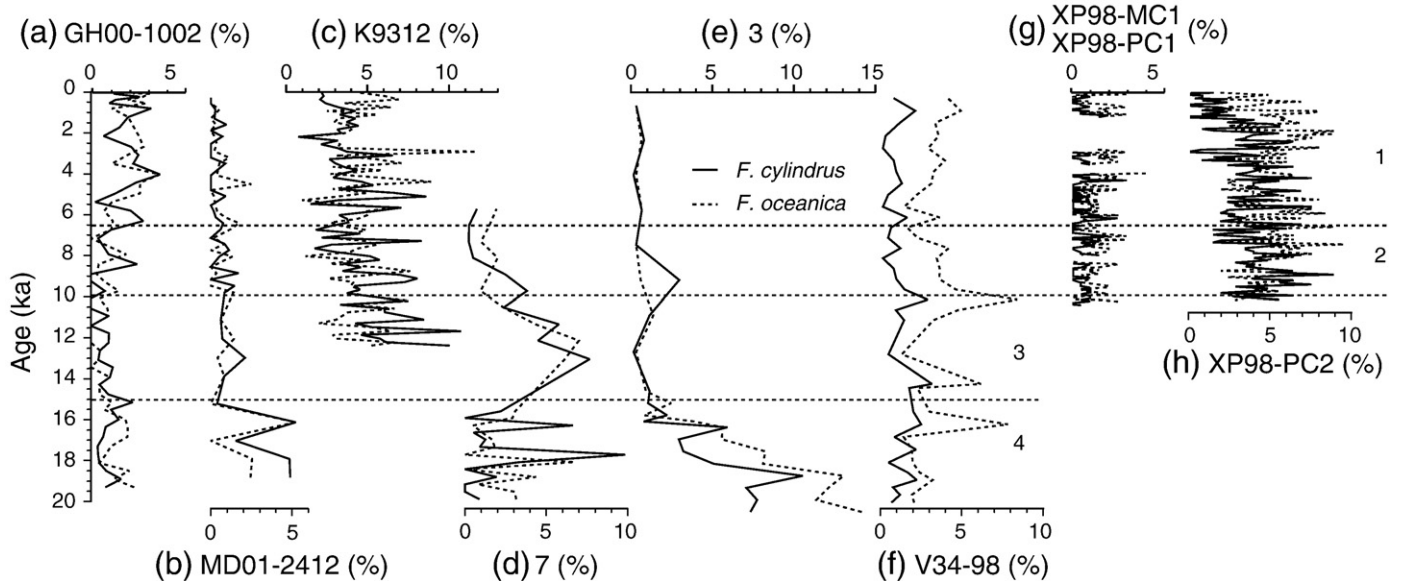


**Fig. 3.** Temporal variation in relative abundances of *Fragilariopsis cylindrus* and *F. oceanica* in core sediments. (a) GH00-1002, (b) MD01-2412, (c) K9312, (d) 7, (e) 3, (f) V34-98, (g) XP98-MC1 and XP98-PC1, and (h) XP98-PC2. Some figures were modified from Shiga and Koizumi (2000), and Koizumi et al. (2003). Location of core can be referred to Fig. 1. Temporal stage can be referred to Fig. 2.

**Table 1**

Data sources of diatom, radiolarian, and ice-rafted debris (IRD) of the Okhotsk Sea sediment cores used in this study.

Diatom		Radiolaria		IRD	
Core name	Data source	Core name	Data source	Core name	Data source
GH00-1002	This paper	GH00-1002	Itaki et al. (2008)	MD01-2412	Sakamoto et al. (2006)
MD01-2412	Okazaki et al. (2005)	GH00-0001	Itaki et al. (2008)	XP98-PC1	Sakamoto et al. (2005)
K9312	Shiga and Koizumi (2000)	GH00-1006	Itaki et al. (2008)	XP98-PC2	Sakamoto et al. (2005)
7	Shiga and Koizumi (2000)	GH001-1011	Itaki et al. (2008)	XP98-PC4	Sakamoto et al. (2005)
3	Shiga and Koizumi (2000)	MD01-2412	Okazaki et al. (2005)	LV28-41-5	Gorbarenko et al. (2003)
V34-98	Shiga and Koizumi (2000)	LV28-42-4	Matul and Abelmann (2001)	936	Gorbarenko et al. (2004)
XP98-MC1	Koizumi et al. (2003)	LV27-5-3	Matul et al. (2003)		
XP98-PC1	Koizumi et al. (2003)	XP98-PC1	Okazaki et al. (2003, 2006)		
XP98-PC2	Koizumi et al. (2003)	XP98-PC2	Okazaki et al. (2003, 2006)		
89211	Gorbarenko et al. (2007a)	XP98-PC4	Okazaki et al. (2003, 2006)		
HO76-P1	Shimada et al. (2004)				

discussion on the relative abundance of *F. cylindrus* and *F. oceanica* in this study.

During the glacial period, the distribution of ice-rafted terrigenous particles indicated no year-round ice cover in the Okhotsk Sea except for the northwestern area (Gorbarenko et al., 2003; Sakamoto et al., 2005, 2006). Based on the high relative abundances of *F. cylindrus* and *F. oceanica* (Fig. 3), sea-ice coverage was deemed to have strongly expanded into the central Okhotsk Sea (core 3; Shiga and Koizumi, 2000) and the coastal area of the southern Okhotsk Sea (cores GH00-1002 and MD01-2412) during the LGM (zone 4). These results correspond to the IRD data of core XP98-PC2 (Sakamoto et al., 2005), core MD01-2412 (Sakamoto et al., 2006), core LV28-41-5 (Gorbarenko et al., 2003), and core 936 (Gorbarenko et al., 2004). However, low abundances of these taxa were reported in core V34-98 during the same period (Fig. 3f; Shiga and Koizumi, 2000). This suggests that seasonal sea-ice basically did not cover the eastern Okhotsk Sea (Fig. 5a). In contrast, several spikes of IRD abundance occurred in core XP98-PC1 in the eastern Okhotsk Sea during the glacial period (Sakamoto et al., 2005). Therefore, it is quite likely that sea-ice only occasionally expanded into the eastern Okhotsk Sea even in the glacial period (zone 4).

The effect of sea-ice increased in the northern central Okhotsk Sea (core 7; Fig. 3d; Shiga and Koizumi, 2000) during the deglacial period between 15 and 10 ka (zone 3). On the northern continental shelf

(core 89211 in Fig. 1; Gorbarenko et al., 2007a), the maximal abundances of *F. cylindrus* and *F. oceanica* were identified at about 10 ka. However, the effect of sea-ice in central and southern Okhotsk Sea between 15 and 10 ka was weaker than during the LGM (cores 3, GH00-1002, and MD01-2412). Such changes in sea-ice taxa are supported by alkenone results. Low alkenone concentrations based on surface-water temperature were measured in central (XP98-PC-2 and XP98-PC-4 in Fig. 1; Seki et al., 2004b) and southern Okhotsk Sea (MD01-2412; Harada et al., 2006) during this period because alkenone production season shifted from mid-summer to autumn as a result of reduction in sea-ice coverage period. This indicates that sea-ice coverage expanded over the northern Okhotsk Sea between 15 and 10 ka, but retreated from the southern Okhotsk Sea during the same period (Fig. 5b). However, it should be emphasized that core 89211 was collected from the relatively shallow depth of about 140 m (Gorbarenko et al., 2007a). It is quite likely that variations of sea-ice taxa in core 89211 reflected local geographic changes. Thus, further investigation is necessary to fully ascertain detailed historical sea-ice distribution on the northern continental shelf.

Relative abundance of sea-ice taxa in the Okhotsk Sea was reduced on the northern continental shelf (core 89211), and was still low in the southern Okhotsk Sea (cores GH00-1002 and MD01-2412) between 10 and 6.5 ka (zone 2). However, sea-ice taxa abundance was still high or increased in the western (core K9312; Shiga and Koizumi, 2000), central (core 7), and eastern (V34-98) Okhotsk Sea between 10 and 8 ka (Fig. 3). Sea-ice taxa diminished in these regions after 8 ka. The frequency and durations of sea-ice coverage extended to the southern central Okhotsk Sea during the first half of this period (Fig. 5c), and subsequently retreated from the central area since 8 ka. The IRD data of cores XP98-PC1, -PC2, and PC-4, located along the east–west transect in the central Okhotsk Sea, also indicate such regression of sea-ice at around 8 ka (Sakamoto et al., 2005).

Sea-ice conditions have been the same since 6.5 ka (zone 1) to the present-day level (Fig. 5d). Contrary to sea-ice distribution between 10 and 6.5 ka, the distributions of sea-ice related to diatom taxa were large in the northern and southern Okhotsk Sea, but small in the western and central Okhotsk Sea (Fig. 3, HO76-P1: Shimada et al., 2004). In the eastern Okhotsk Sea, the relative abundance of sea-ice diatom was high in core V34-98 (Fig. 3f), while IRD has also been high in core XP98-PC1 (Sakamoto et al., 2005). According to Sakamoto et al. (2005), sea-ice in the eastern Okhotsk Sea drifted from the Kamchatka Peninsula during this period.

## 5.2. Atmospheric pressure patterns based on radiolaria and sea-ice distribution

Although sea-ice distribution in the Okhotsk Sea is controlled by discharge from the Amur River (Ogi and Tachibana, 2006), the atmospheric pressure pattern is a more dominant factor (e.g., Ohshima et al., 2006). Sea-ice formation in polynyas of the northern

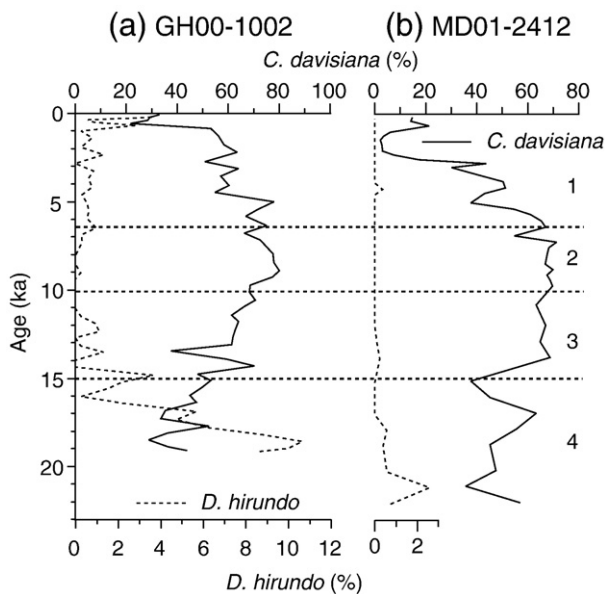


**Fig. 4.** Temporal variation in relative abundances of *Cycladophora davisiana* and *Dityophimus hirundo* in core sediments. (a) GH00-1002 and (b) MD01-2412. Temporal stage can be referred to Fig. 2.

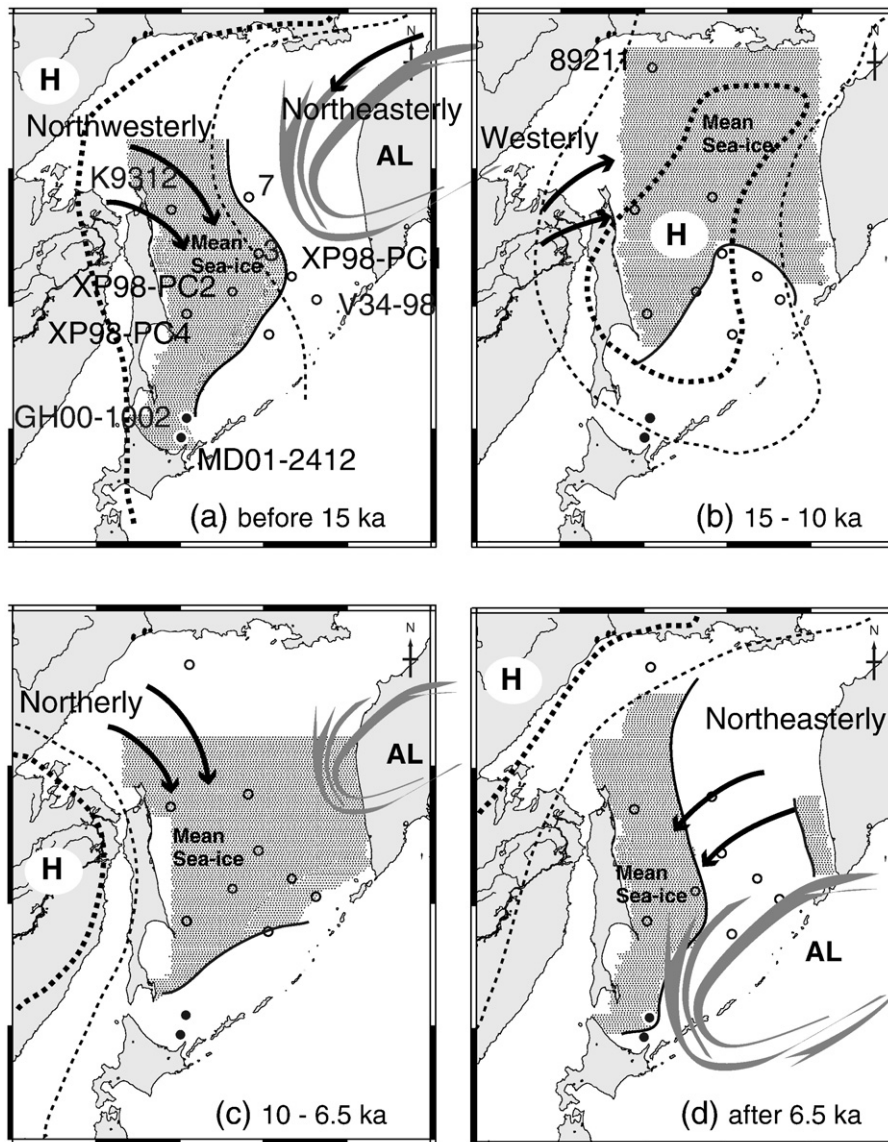


**Fig. 5.** A schematic illustration depicting the distribution of sea-ice distribution and the atmospheric pressure patterns over the Okhotsk Sea since the LGM. (a) Zone 4 (before 15 ka); southern Aleutian Low mode, (b) zone 3 (15–10 ka); strong Siberian High mode, (c) zone 2 (10–6.5 ka); northern Aleutian Low mode, and (d) zone 1 (after 6.5 ka); southern Aleutian Low mode.

continental shelf of the Okhotsk Sea is governed by wind direction and strength in winter (Martin et al., 1998; Kimura and Wakatsuchi, 2004). Wind direction and strength depend on winter atmospheric circulations, such as the geostrophic wind associated with the AL position (Rikiishi and Takatsuji, 2005). The low air temperature over northern Eurasia is related to the intensification and anomalously southward shift of AL pressure system, and the negative phase of the Arctic Oscillation (e.g., Wu and Wang, 2002). When AL shifts southward, the prominent easterly wind reduces polynya development in the northern continental shelf, while area of sea-ice cover is also diminished in the central Okhotsk Sea. In contrast, northerly winds are intensified when the position of AL pressure shifts to the north, resulting in expansion of polynyas in the northern continental shelf of the Okhotsk Sea (Kimura and Wakatsuchi, 2004). As a result, the area of sea-ice cover increases over the Okhotsk Sea (Martin et al., 1998). Therefore, the history of pressure patterns over the Okhotsk Sea can be traced through sea-ice distribution in the Okhotsk Sea.

Relative abundances of diatom assemblages during the LGM and strong sea-ice expansion into the central Okhotsk Sea indicate the frequent occurrence of northern AL mode (Fig. 5a). Northwesterly

geostrophic wind should expand sea-ice distribution into the central Okhotsk Sea. However, northwesterly winds along the northern AL prevent the sea-ice expansion to the northern and eastern Okhotsk Sea. This interpretation is also supported by radiolarian data. Based on *C. davisiana* abundance record in cores GH00-1002 and MD01-2412 (Fig. 4), OSIW had been well ventilated before 15 ka compared to the present-day (Itaki and Ikehara, 2004; Itaki et al., 2008). Radiolarian *C. davisiana* lives abundantly in intermediate water depth (200–500 m) in the Okhotsk Sea (Nimmergut and Abelmann, 2002). This species has been regarded as a tracer of cold and well-oxygenated intermediate water such as the OSIW (Ohkushi et al., 2003; Abelmann and Nimmergut, 2005), and its abundance partially reflects bacterial biomass in the intermediate water mass (Okazaki et al., 2004). Studies in the central Okhotsk Sea (e.g., Matul and Abelmann, 2001; Matul et al., 2003; Gorbarenko et al., 2004) also identified the well ventilated intermediate water during the LGM. *C. davisiana* records proposed that OSIW formation was more active during the LGM than the present-day under the northern AL mode. Nonetheless, our interpretation contradicts the explanation of Ohkushi et al. (2003), suggesting less production of the OSIW during the LGM, based on less *C. davisiana*



have increased suddenly at around 2 ka following the pressure pattern change, which weakened the formation of the OSIW.

## 6. Conclusions

Observation of microfossil assemblages indicate that paleoenvironmental changes are closely related to sea-ice distribution and atmospheric circulation pattern in the southwestern Okhotsk Sea since the LGM.

- (1) Before 15 ka (zone 4): duration of sea-ice cover has been long and sea-ice expanded into the central and southern Okhotsk Sea, owing to frequent occurrence of northern AL mode.
- (2) 15–10 ka (zone 3): sea-ice expanded in the northern Okhotsk Sea, whereas it retreated from the southern Okhotsk Sea. Such distribution of sea-ice was governed by the pronounced westerly winds under strong SH mode, which favors the development of extensive polynyas on the northern continental shelf of the Okhotsk Sea, forming the OSIW.
- (3) 10–6.5 ka (zone 2): sea-ice distribution expanded into the eastern Okhotsk Sea. Occurrence of northern AL mode became more frequent. However, the AL was weak and/or located eastward, compared with it before 15 ka, and resulting in the accelerated formation of the OSIW.
- (4) 6.5 ka–present (zone 1): sea-ice distribution has not fluctuated too much, and the atmospheric pressure pattern has settled to what we can be seen in the present-day, characterized by increasing frequency of southern AL mode. However, OSIW formation became weakened at around 2 ka due to strong runoff from the Amur and other rivers.

## Acknowledgements

We sincerely thank the captain, crews, and scientists on board the IMAGES WEPAMA 2001 Cruise of R/V Marion Defresne and R/V Hakurei-maru No. 2 of the Geological Survey of Japan for their assistance in core sampling. Editor, Tom Cronin and two anonymous reviewers are appreciated on improving the interpretation of our data. This research was made possible by financial support from Korea Institute of Marine Science and Technology Promotion (International Collaboration Research Program; Grant No. 2008001024), by the Ministry of Land, Transport and Maritime Affairs, Korea Polar Research Institute (Grant No. PE10010), and the Geological Survey of Japan.

## References

Abelmann, A., Nimmergut, A., 2005. Radiolarians in the Sea of Okhotsk and their ecological implication for paleoenvironmental reconstructions. *Deep-Sea Res. II* 52, 2302–2331.

Alfultis, M.A., Martin, S., 1987. Satellite passive microwave studies of the Sea of Okhotsk ice cover and its relation to oceanic processes, 1978–1982. *J. Geophys. Res.* 92, 13013–13029.

Cremer, H., 1999. Distribution patterns of diatom surface sediment assemblages in the Laptev Sea (Arctic Ocean). *Mar. Micropaleontol.* 38, 39–67.

Gorbarenko, S.A., 1996. Stable isotope and lithologic evidence of late-glacial and Holocene oceanography of the northwestern Pacific and its marginal sea. *Quat. Res.* 46, 230–250.

Gorbarenko, S.A., Leskov, V.Y., Artemova, A.V., Tiedemann, R., Biebow, N., Nuernberg, D., 2003. Ice Cover in the Sea of Okhotsk during the Last Glaciation and Holocene. *Dokl. Earth Sci.* 389, 208–211.

Gorbarenko, S.A., Southon, J.R., Keigwin, L.D., Cherepanova, M.V., Gvozdeva, I.G., 2004. Late Pleistocene–Holocene oceanographic variability in the Okhotsk Sea: geochemical, lithological and paleontological evidence. *Palaeogeogr. Palaeoclimatol. Palaeoecol.* 209, 281–301.

Gorbarenko, S.A., Tsoi, I.B., Astakhov, A.S., Artemova, A.V., Gvozdeva, I.G., Annin, V.K., 2007a. Paleoenvironmental changes in the northern shelf of the Sea of Okhotsk during the Holocene. *Stratigr. Geol. Correl.* 15, 656–671.

Gorbarenko, S.A., Goldberg, E.L., Kashgarian, M., Velivetskaya, T.A., Zakharkov, S.P., Pechnikov, V.S., Bosin, A.A., Psheneva, O.Y., Diamilevnaivanova, E., 2007b. Millennium scale environment changes of the Okhotsk Sea during last 80 kyr and their phase relationship with global climate changes. *J. Oceanogr.* 63, 609–623.

Harada, N., Ahagon, N., Sakamoto, T., Uchida, M., Ikehara, M., Shibata, Y., 2006. Rapid fluctuation of alkenone temperature in the southwestern Okhotsk Sea during the past 120 ky. *Global Planet. Change* 53, 29–46.

Hasle, G.R., 1990. Arctic plankton diatoms: dominant species, biogeography. In: Medlin, L.K., Priddle, J. (Eds.), *Polar marine Diatoms*. British Antarctic Survey, Cambridge, pp. 53–56.

Hasle, G.R., Syvertsen, E.E., 1996. Marine diatoms. In: Tomas, C.R. (Ed.), *Identifying Marine Phytoplankton*. Academic Press, California, pp. 5–386.

Horner, R., Alexander, V., 1972. Algal populations in Arctic sea-ice: an investigation of heterotrophy. *Limnol. Oceanogr.* 17, 454–458.

Itaki, T., 2006. Elutriation technique for extracting radiolarian skeletons from sandy sediments and its usefulness for faunal analysis. *Radiolaria* 24, 14–18.

Itaki, T., Ikehara, K., 2004. Middle to late Holocene changes of the Okhotsk Sea Intermediate Water and their relation to atmospheric circulation. *Geophys. Res. Lett.* 31 (Art. No. L24309).

Itaki, T., Khim, B.K., Ikehara, K., 2008. Last glacial–Holocene water structures in the southwestern Okhotsk Sea inferred from radiolarian assemblages. *Mar. Micropaleontol.* 67, 191–215.

Itoh, M., Ohshima, K.I., Wakatsuchi, M., 2003. Distribution and formation of Okhotsk Sea Intermediate Water: an analysis of isopycnal climatological data. *J. Geophys. Res.* 108 (C8), 3258. doi:10.1029/2002JC001590.

Kawahata, H., Ohshima, H., Shimada, C., Oba, T., 2003. Terrestrial–oceanic environmental change in the southern Okhotsk Sea during the Holocene. *Quat. Int.* 108, 67–76.

Kawamura, N., Oda, H., Ikehara, K., Yamazaki, T., Shioi, K., Taga, S., Hatakeyama, S., Torii, M., 2007. Diagenetic effect on magnetic properties of marine core sediments from the southern Okhotsk Sea. *Earth Planets Space* 59, 83–93.

Keigwin, L.D., 1998. Glacial-age hydrography of the far northwest Pacific Ocean. *Paleoceanography* 13, 323–339.

Keigwin, L.D., 2002. Late Pleistocene–Holocene paleoceanography and ventilation of the Gulf of California. *J. Oceanogr.* 58, 421–432.

Kimura, N., Wakatsuchi, M., 2004. Increase and decrease of sea ice area in the Sea of Okhotsk: ice production in coastal polynyas and dynamic thickening in convergence zones. *J. Geophys. Res.* 109, C09S03. doi:10.1029/2003JC001901.

Koizumi, I., Shiga, K., Irino, T., Ikehara, M., 2003. Diatom record of the late Holocene in the Okhotsk Sea. *Mar. Micropaleontol.* 49, 139–156.

Kutzbach, J.E., 1970. Large-scale features of monthly mean northern hemisphere anomaly map of sea-level pressure. *Mon. Weather Rev.* 98, 708–716.

Martin, S., Drucker, R., Yamashita, K., 1998. The production of ice and dense shelf water in the Okhotsk Sea polynyas. *J. Geophys. Res.* 103, 27771–27782.

Matul, A.G., Abelmann, A., 2001. Quaternary water structure of the Sea of Okhotsk based on radiolarian data. *Dokl. Earth Sci.* 38, 1005–1007.

Matul, A.G., Gorbarenko, S.A., Mukhina, V.V., Leskov, V.Yu., 2003. The Quaternary micropaleontological and lithophysical records in the sediments of the northern part of the Sea of Okhotsk. *Oceanology* 43, 551–560.

Morley, J.J., Heusser, L.E., Shackleton, N.J., 1991. Late Pleistocene/Holocene radiolarian and pollen records in the Sea of Okhotsk. *Paleoceanography* 6, 121–131.

Narita, H., Sato, M., Tsunogai, S., Murayama, M., Ikehara, M., Nakatsuka, T., Wakatsuchi, M., Harada, N., Ujiie, Y., 2002. Biogenic opal indicating less productive northwestern North Pacific during the glacial ages. *Geophys. Res. Lett.* 29 10.1029/2001GL014320.

Nimmergut, A., Abelmann, A., 2002. Spatial and seasonal changes of radiolarian standing stocks in the Sea of Okhotsk. *Deep-Sea Res.* 49, 463–493.

Ogi, M., Tachibana, Y., 2006. Influence of the annual Arctic Oscillation in the negative correlation between Okhotsk Sea ice and Amur River discharge. *Geophys. Res. Lett.* 33, L086709. doi:10.1029/2006GL025838.

Ohkushi, K., Itaki, T., Nemoto, N., 2003. Last Glacial–Holocene change in intermediate-water ventilation in the Northwestern Pacific. *Quat. Sci. Rev.* 22, 1477–1484.

Ohshima, K., Nihashi, S., Hashiya, E., Watanabe, T., 2006. Interannual variability of sea ice area in the Sea of Okhotsk: importance of surface heat flux in fall. *J. Meteorol. Soc. Jpn.* 84, 907–919.

Okazaki, Y., Takahashi, K., Yoshitani, H., Nakatsuka, T., Ikehara, M., Wakatsuchi, M., 2003. Radiolarians under the seasonally sea-ice covered conditions in the Okhotsk Sea: flux and their implications for paleoceanography. *Mar. Micropaleontol.* 49, 195–230.

Okazaki, Y., Takahashi, K., Itaki, T., Kawasaki, Y., 2004. Comparison of radiolarian vertical distributions in the Okhotsk Sea near the Kuril Islands and in the northwestern North Pacific off Hokkaido Island. *Mar. Micropaleontol.* 51, 257–284.

Okazaki, Y., Takahashi, K., Katsuki, K., Ono, A., Hori, J., Sakamoto, T., Uchida, M., Shibata, Y., Ikehara, M., Aoki, K., 2005. Late Quaternary paleoceanographic changes in the southwestern Okhotsk Sea: evidence from geochemical, radiolarian, and diatom records. *Deep-Sea Res. II* 52, 2332–2350.

Okazaki, Y., Seki, O., Nakatsuka, T., Sakamoto, T., Ikehara, M., Takahashi, K., 2006. *Cycladophora davisiana* (Radiolaria) in the Okhotsk Sea: a key for reconstructing glacial ocean conditions. *J. Oceanogr.* 62, 639–648.

Overland, J.E., Adams, J.M., Bond, N.A., 1999. Decadal variability of the Aleutian Low and its relation to high-latitude circulation. *J. Climate* 12, 1542–1548.

Rikiishi, K., Takatsuki, S., 2005. On the growth of ice cover in the Sea of Okhotsk with special reference to its negative correlation with that in the Bering Sea. *Ann. Glaciol.* 42, 380–388.

Sakamoto, T., Ikehara, M., Aoki, K., Iijima, K., Kimura, N., Nakatsuka, T., Wakatsuchi, M., 2005. Ice-rafted debris (IRD)-based sea-ice expansion events during the past 100 kyrs in the Okhotsk Sea. *Deep-Sea Res. II* 52, 2275–2301.

Sakamoto, T., Ikehara, M., Uchida, M., Aoki, K., Shibata, Y., Kanamatsu, T., Harada, N., Iijima, K., Katsuki, K., Asahi, H., Takahashi, K., Sakai, H., Kawahata, H., 2006. Millennial-scale variations of sea-ice expansion in the southwestern part of the

- Okhotsk Sea during the past 120 kyr: age model and ice-rafted debris in IMAGES core MD01-2412. *Global Planet. Change* 53, 58–77.
- Sancetta, C., 1982. Distribution of diatom species in surface sediment of the Bering and Okhotsk Seas. *Micropaleontology* 28, 221–257.
- Sancetta, C., 1983. Effect of Pleistocene glaciation upon oceanographic characteristics of the North Pacific Ocean and Bering Sea. *Deep-Sea Res.* 30, 851–869.
- Seki, O., Kawamura, K., Nakatsuka, T., Ohnishi, K., Ikehara, M., Wakatsuchi, M., 2003. Sediment core profiles of long-chain n-alkanes in the Sea of Okhotsk: enhanced transport of terrestrial organic matter from the last deglaciation to the early Holocene. *Geophys. Res. Lett.* 30, 1001. doi:10.1029/2001GL014464.
- Seki, O., Ikehara, M., Kawamura, K., Nakatsuka, T., Ohnishi, K., Wakatsuchi, M., Narita, H., Sakamoto, T., 2004a. Reconstruction of paleoproductivity in the Sea of Okhotsk over the last 30 kyr. *Paleoceanography* 19, 1016. doi:10.1029/2002PA000808.
- Seki, O., Kawamura, K., Ikehara, M., Nakatsuka, T., Oba, T., 2004b. Variation of alkenone sea surface temperature in the Sea of Okhotsk over the last 85 kyr. *Org. Geochem.* 35, 347–354.
- Shiga, K., Koizumi, I., 2000. Latest Quaternary oceanographic changes in the Okhotsk Sea based on diatom records. *Mar. Micropaleontol.* 38, 91–117.
- Shimada, C., Ikehara, K., Tanimura, Y., Hasegawa, S., 2004. Millennial-scale variability of Holocene hydrography in the southwestern Okhotsk Sea: diatom evidence. *Holocene* 14, 641–650.
- Smith, L.M., Miller, G.H., Otto-Bliesner, B., Shin, S., 2003. Sensitivity of the Northern Hemisphere climate system to extreme changes in Holocene Arctic sea ice. *Quat. Sci. Rev.* 22, 645–658.
- Sorokin, Y.I., Sorokin, P.I., 1999. Production in the Sea of Okhotsk. *J. Plankton Res.* 22, 201–230.
- Talley, L.D., 1991. An Okhotsk Sea water anomaly: implications for ventilation in the North Pacific. *Deep-Sea Res.* 38, S171–S190.
- Ternois, Y., Kawamura, K., Keigwin, L.D., Ohkouchi, N., Nakatsuka, T., 2001. A biomarker approach for assessing marine and terrigenous inputs to the sediments of Sea of Okhotsk for the last 27,000 years. *Geochim. Cosmochim. Acta* 65, 791–802.
- Watanabe, T., Wakatsuchi, M., 1998. Formation of 26.8–26.9  $\sigma_{\theta}$  water in the Kuril Basin of the Sea of Okhotsk as a possible origin of North Pacific Intermediate Water. *J. Geophys. Res.* 103, 2849–2865.
- Wong, C.S., Matear, R.J., Freeland, H.J., Whitney, F.A., Bychkov, A.S., 1998. WOCE line P1W in the Sea of Okhotsk 2. CFCs and the formation rate of intermediate water. *J. Geophys. Res.* 103, 15625–15642.
- Wu, B., Wang, J., 2002. Winter Arctic Oscillation, Siberian High and east Asian winter monsoon. *Geophys. Res. Lett.* 29, 1897. doi:10.1029/2002GL015373.
- Yamamoto, M., Suemune, R., Oba, T., 2005. Equatorward shift of the subarctic boundary in the northwestern Pacific during the last deglaciation. *Geophys. Res. Lett.* 32, L05609. doi:10.1029/2004GL021903.
- Yasuda, I., 1997. The origin of the North Pacific Intermediate Water. *J. Geophys. Res.* 102, 893–909.